Theor Appl Climatol (2018) 131:153–165
DOI 10.1007/s00704-016-1965-9

ORIGINAL PAPER

# Bark beetle-induced tree mortality alters stand energy budgets due to water budget changes

**David E Reed**[1,2,3] · **Brent E Ewers**[2,3,4] · **Elise Pendall**[2,3,4] · **John Frank**[2,3,4,5] · **Robert Kelly**[2,4,6]

Received: 24 July 2015 / Accepted: 7 October 2016 / Published online: 19 October 2016


**Abstract** Insect outbreaks are major disturbances that affect a land area similar to that of forest fires across North America. The recent mountain pine bark beetle (*Dendroctonus ponderosae*) outbreak and its associated blue stain fungi (*Grosmannia clavigera*) are impacting water partitioning processes of forests in the Rocky Mountain region as the spatially heterogeneous disturbance spreads across the landscape. Water cycling may dramatically change due to increasing spatial heterogeneity from uneven mortality. Water and energy storage within trees and soils may also decrease, due to hydraulic failure and mortality caused by blue stain fungi followed by shifts in the water budget. This forest disturbance was unique in comparison to fire or timber harvesting because water fluxes were altered before significant structural change occurred to the canopy. We investigated the impacts of bark beetles on lodgepole pine (*Pinus contorta*) stand and ecosystem level hydrologic processes and the resulting vertical and horizontal spatial variability in energy storage. Bark beetle-impacted stands had on average 57 % higher soil moisture, 1.5 °C higher soil temperature, and 0.8 °C higher tree bole temperature over four growing seasons compared to unimpacted stands. Seasonal latent heat flux was highly correlated with soil moisture. Thus, high mortality levels led to an increase in ecosystem level Bowen ratio as sensible heat fluxes increased yearly and latent heat fluxes varied with soil moisture levels. Decline in canopy biomass (leaf, stem, and branch) was not seen, but ground-to-atmosphere longwave radiation flux increased, as the ground surface was a larger component of the longwave radiation. Variability in soil, latent, and sensible heat flux and radiation measurements increased during the disturbance. Accounting for stand level variability in water and energy fluxes will provide a method to quantify potential drivers of ecosystem processes and services as well as lead to greater confidence in measurements for all dynamic disturbances.

✉ David E Reed
David.Edwin.Reed@gmail.com

[1] Department of Atmospheric and Oceanic, University of Wisconsin, 1225 W. Dayton Street, Madison, WI 53706, USA

[2] Program in Ecology, University of Wyoming, 1000 E. University, Laramie, WY 82071, USA

[3] Hawkesbury Institute for the Environment, University of Western Sydney, Locked Bag 1701, Penrith, Sydney, NSW 2571, Australia

[4] Department of Botany, University of Wyoming, 1001 E. University, Laramie, WY 82071, USA

[5] US Forest Service, Rocky Mountain Research Station, 240 West Prospect, Fort Collins, CO 80526, USA

[6] Department of Atmospheric Science, University of Wyoming, 1001 E. University, Laramie, WY 82071, USA

## 1 Introduction

Forest mortality is increasing worldwide in recent decades (Allen et al. 2010; van Mantgem et al. 2009). An increase in both extreme heat and drought stress in the coming decades is hypothesized to decrease forest resistance to other stressors (Niinemets 2010), including air pollutants and nitrogen (McNulty et al. 1996) and ozone deposition (Panek et al. 2002; Tingey et al. 2001). Additionally, global warming is increasing fire frequency in forests (Flannigan et al. 2005; Minckley et al. 2012; Tymstra et al. 2007; Westerling et al. 2006). Insect outbreaks, including budworms (Bergeron et al. 1995), forest tent caterpillars (Man and Rice 2010), and bark beetles (Edburg et al. 2012; Kurz et al. 2008b; Raffa et al. 2008), are altering forest composition, biogeochemical cycling, and function.

Insect disturbance directly increases forest heterogeneity (Turner 1989) and can have wide-ranging effects including radiation distribution throughout canopies (Asrar et al. 1992) and altering mechanisms that control mass exchange (Amiro et al. 2010; Baldocchi et al. 2000; Prescott, 2002) and energy fluxes within ecosystems (Baldocchi et al. 2000). Ecosystem nutrient cycling and water quality are also impacted by disturbances (Mikkelson et al. 2013; Rhoades et al. 2013), which are difficult to generalize due to complex spatial heterogeneity across landscapes (Mikkelson et al. 2013). Understanding how disturbances change biosphere-atmosphere exchange mechanisms is important both for process level understanding and improving predictions of forest response (Edburg et al. 2012; Pugh and Gordon 2013).

The magnitude of the current mountain pine bark beetle outbreak in Western North America is larger than any previously recorded infestation (Kurz et al. 2008a; Raffa et al. 2008; Safranyik et al. 2010). This ongoing bark beetle disturbance first affects the water cycle by causing hydraulic failure within host trees during initial infestation (Hubbard et al. 2013; Yamaoka et al. 1990). This may lead to hydrologic impacts on stream flow at the ecosystem level if the mortality is high (Potts 1984), although recent work has shown no substantial impact on snowpack (Biederman et al. 2014a; Biederman et al. 2015). However, snowpack melt rates can change (Pugh and Small 2012) and overall water cycling results are complex and results are not consistent between studies (Mikkelson et al. 2013).

Eddy covariance methods have become a standard approach to quantify mass and energy fluxes between ecosystems and the lower atmosphere (Baldocchi et al. 2001), with recent studies focused on disturbance effects from mountain pine beetles in British Columbia (Brown et al. 2010; Brown et al. 2012). Bark beetle infestation at the study site (Chimney Park, Wyoming) began in summer 2007 and ecosystem fluxes, stand level temperature, and moisture have been measured since 2009 (Reed et al. 2014). Objectives of this work are to quantify the extent of mortality throughout the initial infestation and test the following hypothesis. (1) Throughout the course of the outbreak, soil water will increase while canopy water will decrease. (2) Surface outgoing shortwave radiation will decrease as the canopy goes from green to gray and then outgoing longwave radiation will increase as more longwave radiation from the warmer soil surface passes through the canopy as the canopy opens. Overall, there will be little change to net radiation. (3) Because of the decrease in tree transpiration, the site's sensible heat and Bowen ratio will increase.

## 2 Methods

### 2.1 Site description

Eddy covariance-based flux measurements of water vapor and energy were conducted at the Chimney Park study site in Medicine Bow Range in Southeast Wyoming (41.37 N, 106.53 W) at 2770 m elevation. The tower footprint is primarily a near-even-aged forest of lodgepole pine (*Pinus contorta*, 81.2 %) with small amounts of aspen (*Populus tremuloides*, 11.2 %), Douglas fir (*Pseudotsuga menziesii*, 5.0 %), and Engelmann spruce (*Picea engelmannii*, 0.8 %). The most recent stand-replacing fire was 135 years ago (Knight et al. 1985), while thinning over the past 40 years has resulted in only a small unmanaged (i.e., unthinned) area with the remaining forest stands having similar canopy heights, nearly closed canopies, and little to no under canopy vegetation before the onset of the current outbreak. Mountain pine beetles (*Dendroctonus ponderosae*) and the associated symbiotic blue stain fungi (*Grosmannia clavigera*) have infected a high proportion of large lodgepole pine trees in the region. Soils were shallow at the site, with >90 % of roots found within 40 cm of the surface (Knight et al. 1985). The soil was classified as a Typic Cryoboralf from granite, amphibolite, and felsic gneiss parent materials (Ponton et al. 2006).

Bark beetles are highly selective on tree bole diameter measured at breast height (DBH) (Negrón and Popp 2004), and individual forest stand measurements of water and energy within the tower footprint are delimited based on year of attack. The selection of beetles leads to common stand condition classes as well as characteristics, primarily DBH and density (Table 1). Stands named based on the first year bark beetles were found in the stand. For example, BB07 first had bark beetles present in 2007. One unthinned stand had smaller DBH and higher tree density than beetle-attacked stands and experienced virtually no beetle infestation (unimpacted stand). For DBH and basal area measurements, each stand had five subplots. Tree condition was categorized in five classes: "dead standing" for trees that died previously to this study from non-beetle causes but remain standing, the "uninfected phase" for no signs of beetle attack, the "beetle green phase" for infested trees but with green needles, the "beetle red phase" for infested trees with red needles, and the "beetle gray phase" when needles began to fall. This is similar to the classification of Pugh and Small (2012). Trees classified as beetle green, beetle red, and beetle gray were all considered as dead within the growing season of measurement. Although beetle green trees were classified as infested, transpiration rates decrease rapidly throughout the early growing season in the year when they are infested (Hubbard et al. 2013; Yamaoka et al. 1990). The surface area of canopy biomass (leaf, steam, and branch), per unit ground area, was measured as the leaf area index (LAI) and multiple repeated measurements were taken with

**Table 1** Average diameter breast height (DBH), leaf area index (LAI), tree density of all tree conditions (not including dead standing trees), and footprint percentage for stands examined in this study (standard error). The LAI values apply to the 2009 season.

| Stand | DBH (cm) | Canopy height (m) | LAI ($m^2$ $m^{-2}$) | Tree density (stems $ha^{-1}$) | Scaled percent of footprint |
|---|---|---|---|---|---|
| BB09 | 14.3 (0.15) | 13.2 (0.30) | 2.44 (0.10) | 2531 (14) | 15.8 % |
| BB08 | 24.1 (0.29) | 18.6 (0.54) | 2.34 (0.13) | 1013 (6) | 40.0 % |
| BB07 | 21.9 (0.34) | 18.3 (0.38) | 1.80 (0.24) | 600 (22) | 40.0 % |
| Unimpacted | 7.5 (0.17) | 12.05 (0.61) | 2.91 (0.28) | 17,556 (145) | 4.2 % |

a plant canopy analyzer (LAI-2000; Li-Cor Inc., USA) at five randomly selected points in each stand over several days in 2009.

Vegetation characteristics within the entire 800-m by 450-m tower footprint that is described below were sampled following Burrows et al. (2002)) with a cyclic sampling grid of 15 repeated 175-m by 150-m blocks spaced as a 3-m × 5-m rectangle. Sampling blocks were each subsampled at 0, 25, and 75 m for a total of 106 plots. This provides an efficient way to measure spatial variability of parameters with individual sample plots being separated from neighboring plots by multiple distances. Access issues prevented sampling in one footprint corner. Cyclically sampled grid data were collected August 17 and 26, 2010. These plots were compared with replicated stand level DBH, basal area, tree condition, and mortality data from the same time period and located within the cyclic grid, in order to scale four instrumented stands to the entire footprint by a "paint-by-numbers" approach (Burrows et al. 2002; Mackay et al. 2002).

Over the years 2009–2012, mean annual temperature was 6.1 °C; monthly average temperatures varied from −7.3 °C in January to 14.6 °C in August. Average precipitation was 662 mm with only 264 mm of precipitation in the summer months (Biederman et al. 2014b). Maximum snow accumulation of 28.6 cm snow water equivalent (SWE) in 2010 and 27.0 cm SWE in 2011 based on measurements approximately 1 week before the snowpack turned isothermal (Biederman et al. 2014a). 2012 was a particularly dry year (Hoerling et al. 2014), with a 32 % reduction of annual precipitation to 448 mm (125 mm summer precipitation) and SWE of 26.6 cm. Snow melt typically occurred during late April or May, with soils being fully saturated at the conclusion of snowmelt in 2010 and 2011, as evidenced by soil moisture probes, soil pit observations, and shallow surface ponding lasting 5–10 days after the end of snowmelt (J. Biederman, personal communication).

### 2.2 Sensible and latent heat flux measurements

An 18-m eddy covariance tower was located within BB09, with stand and eddy covariance instruments running at the field site since January 17, 2009. The tower was equipped with an open path infrared gas analyzer (IRGA) (LI-7500; Li-Cor Inc., USA), which measures $CO_2$ and water vapor gas densities, and with a sonic anemometer (CSAT3; Campbell Scientific Inc., USA), which measures three-dimensional wind velocity and air temperature, both at 17.7 m height. A four-component radiometer (CNR1; Kipp & Zonen, the Netherlands) was mounted at a lower height but still above the canopy (17.1 m). Temperature and relative humidity were measured above (17.7 m) and below (3.7 m) canopy (HMP45A; Vaisala, Finland). Photosynthetic photon flux density (PPFD) was measured with a quantum sensor (LI-190; Li-Cor Inc., USA) at a height of 16.7 m. Data signals were recorded at 10 Hz for fast response eddy covariance instruments (LI-7500, CSAT3) with a digital data logger (CR5000; Campbell Scientific Inc., USA). Other sensors were recorded using digital data loggers (CR1000 and CR10X; Campbell Scientific Inc., USA) as 30-min averages.

Ecosystem flux data were processed following standard practice outlined in Lee et al. (2004). These include despiking data (Frank et al. 2014), correction from calibration drifts (Loescher et al. 2009), spatially separate sensor correction (Horst and Lenschow 2009), planar fitting (Finnigan et al. 2003), spectral corrections (Horst 2000; Massman 2000), and the Webb-Pearman-Leuning density fluctuation correction (Webb et al., 1980). A friction velocity threshold of 0.089 m $s^{-1}$ was established using a statistically blind test of Gu et al. (2005) which due to low site turbulence only 1.37 % of the data was removed.

The Bowen ratio ($\beta$) was defined as the ratio of sensible heat flux ($H$) to latent heat flux (LE) as proposed by Bowen (1926) (Eq. 1):

$$\beta = \frac{H}{\mathrm{LE}} \tag{1}$$

A model based on average friction velocity, sensor height, zero plane displacement, and roughness (Monin and Obukhov, 1954; Schuepp et al., 1990) was used to determine the distance from the instrumented flux tower that would comprise the tower's footprint. The study site is 35 ha in size, with a maximum straight line distance of flux contribution of 875 m. The stands used in the study area (Table 1) were chosen to be within the 99 % contribution of flux density area under stable atmospheric conditions. Wind directions were almost exclusively from the west, with 95 % of the wind

coming from between southwest (225°) and northwest (315°), and 87 % of the footprint was located west of the tower. The overall slope of the site is less than 2 %. Under neutral stability atmospheric conditions, the flux tower at the site has peak flux density from a distance of 47 m.

### 2.3 Energy storage measurements

Energy balance for the field site was defined with net radiation ($R_n$), measured latent (LE) and sensible ($H$) heat fluxes, soil heat flux ($G$), and energy storage ($J$) at each 30-min time scale (Eq. 2). The net radiation is positive for energy flux toward the surface; the other values are positive for energy leaving the surface.

$$R_n = \mathrm{LE} + H + G + J \tag{2}$$

Energy storage (Eq. 3) was determined from the sensible ($J_a$, Eq. 4) and latent energy ($J_w$, Eq. 5) within canopy, energy storage by soil ($J_g$, Eq. 6), and energy storage within vegetation biomass ($J_v$, Eq. 7) (McCaughey 1985).

$$J = J_a + J_w + J_g + J_v \tag{3}$$

In Eqs. (4)–(7), specific heat of air ($C_P$) and the psychometric constant ($\gamma$) were assumed to be stationary in time while air densities ($\rho$) were assumed to be constant between measurement heights. Measurement height ($z$) was based on sensor height. Air temperature ($T_a$) was measured and vapor pressure ($e$) was calculated from relative humidity below canopy at a height of 3.7 m. Specific heats of soil water and soil solids($C_w$, $C_s$), and soil bulk density ($\rho_s$) were assumed to be stationary in time. Volumetric soil water ($\theta_w$) and soil temperature ($T_s$) were both measured at 10 cm depth ($z_{soil}$), with water mass ($m_{sw}$) assumed to be stationary. Vegetation mass and vegetation water mass $\left(m_{veg}, m_{H_2O}\right)$ were based on lodgepole pine allometric relationships developed in the region (Pearson et al. 1984), and measured wet/dry biomass ratios were estimated from dried biomass weights. Specific heats of vegetation and water $\left(C_{veg}, C_{H_2O}\right)$ and vegetation density ($\rho_{veg}$) were assumed to be stationary in time. Canopy height ($h$) was based on stand height, 16.2 m at the BB07 and BB08 stands, 11.1 m at the BB09 stand, and 8.7 m at the unimpacted stand. Included in the vegetation energy storage term is energy stored by water mass (Meyers and Hollinger 2004). Vegetation temperature ($T_{veg}$) was measured at breast height (1.3 m).

$$J_a = \rho\, C_P\, T_a\, z \tag{4}$$

$$J_w = \frac{\rho\, C_P\, e\, z}{\gamma} \tag{5}$$

$$J_g = G_{(z_{soil})} + \left(\theta_w\, m_{sw}\, C_w + \rho_s\, C_s\right) T_s\, z_{soil} \tag{6}$$

$$J_v = \left(m_{veg}\, C_{veg} + m_{H_2O}\, C_{H_2O}\right) T_{veg}\, h \tag{7}$$

Each stand (BB07, BB08, BB09, and the unimpacted stand) had one instrumented profile of soil moisture and heat storage installed during October 2009. Soil temperature profiles were recorded with copper-constantan thermocouples at depths of 10, 20, 30, 50, and 70 cm. Soil moisture probes were 30 cm in length (CS616; Campbell Scientific Inc., USA) were deployed to integrate soil water content over depths of 0 to 15, 15 to 45, and 45 to 75 cm. At BB09, two self-calibrating soil heat flux plates (HFP01SC; Hukseflux, Netherlands) were installed at a depth of 5 cm and were paired with a water content reflectometer probe (CS616; Campbell Scientific Inc., USA) and two soil thermocouples at that same depth. Bole temperatures were recorded via copper-constantan thermocouples at a height of 1.3 m and a depth of 2 cm into the bole and sealed with silicone. Six infected and six uninfected trees were instrumented at the BB09 stand, and two infected and two uninfected trees were instrumented at the BB07 stand. Air temperature was measured at 17.7 m height at the BB09 stand. Air temperature above canopy was assumed to be similar across all stands at half hour time scales because of high wind speed and turbulence across the study site.

Atmospheric stability $\xi$ was calculated from

$$\xi = \frac{z-d}{L} \tag{8}$$

where $z$ is sensor height (m), $d$ is zero plane displacement height (m), and $L$ is Monin-Obukhov length (m) (Monin and Obukhov 1954). Due to sensor noise, air and soil temperature time series were smoothed by a weighted central difference function before application in energy storage terms.

For this study, stands were grouped based on average tree density and tree diameter for biomass calculations and average tree height was calculated for atmospheric storage. Stand level energy storage measurements from 2010 and 2011 were used with forest inventory and mortality data from 2009 to 2011 to calculate the parameters of the energy storage equations. Scaling from the stand level to the ecosystem level (Table 1) was done with a simple weighted ground area calculation based on average tree diameter of stands compared with diameters measured in 106 plots spanning the entire footprint, as described in Section 2.1 (Burrows et al. 2002).

### 2.4 Water measurement comparison

Stand level water balance was calculated by selecting periods of time between rain events based on the water content

reflectometer probe time series, similar to the work of Ewers et al. (1999), which simplifies water budgets and removes issues of drainage from consideration. Time periods were selected based on shallow (0–15 cm) depth probes. There were a total of 11 periods and the length of each period varied between 7 and 58 days. Total soil water depletion ($\Delta\theta$) was based on an average of shallow and deep (15–45 cm) soil water layers. Due to >90 % of the rooting zone being encompassed in the soil water measurement layers (Ponton et al. 2006) and observations of a perched water table just below rooting depth (J. Biederman, personal communication), soil drainage did not need to be accounted for. Soil water depletion was based on water content differences from start to end of time periods while evapotranspiration was summed over those same time periods. Error in summation of water flux was calculated as standard error over the entire time period between rain events, with daily sums of water flux as individual replicates (Moncrieff et al., 1996). Analysis was restricted to the growing season, defined as May to September. All data were processed using MATLAB (2010a, The MathWorks). Bagplots were created following Rousseeuw et al. (1999).

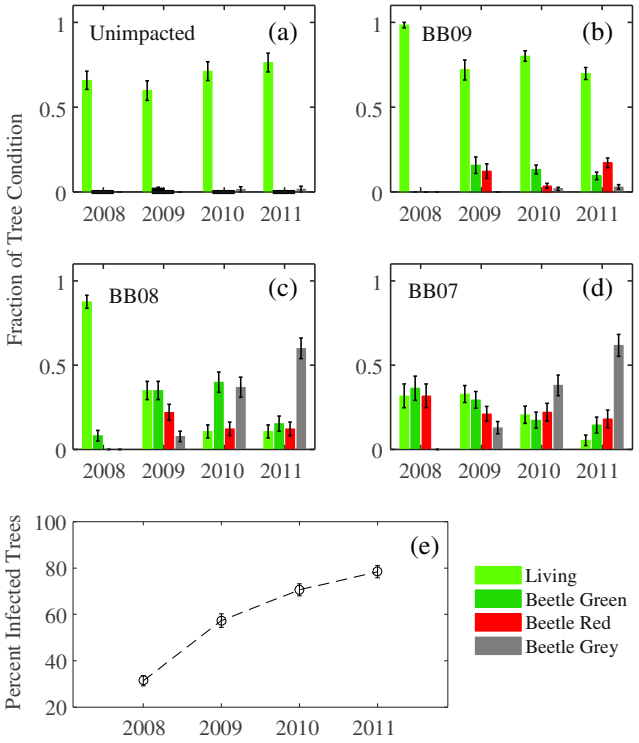


**Fig. 1** Recorded mortality at unimpacted (**a**), BB09 (**b**), BB08 (**c**), and BB07 (**d**) stands for 2008–2011. Mortality by year, spatially scaled by basal area (**e**). *Error bars* for all panels are standard deviations. Not included is the class condition of dead standing, which average 22, 0.7, 0.7, and 1 % between years at the unimpacted, BB09, BB08, and BB07 stands

## 3 Results

### 3.1 Bark beetle-induced mortality

Average tree diameter over the eddy covariance tower footprint was 16.6 cm, ranging from 7.5 to 24.1 cm among stands (Table 1). Tree mortality in the tower footprint was positively correlated to tree diameter, with historical records showing a minimum DBH needed for infestation to be 13 cm (Hopping and Beall 1948). At the end of the study, in plots with an average 7.5 cm DBH, mortality was low (1.0 %); wherein plots with a larger average DBH of 24.1 cm, mortality levels were 94.5 %. We observed an increase of mortality from 30 % in the second year to 78 % by the fourth year following initial infestation, across the entire flux tower footprint (Fig. 1).

During the first 2 years of beetle infestation, there was little to no effect of canopy structure on light interception. Healthy and infected stands had 2.34 (±0.13) LAI (±standard error) and 2.44 (±0.10) $m^2\ m^{-2}$, respectively, while needles were still attached. Only after needles began to fall after two seasons did LAI drop to 1.80 (±0.24) $m^2\ m^{-2}$ (Table 1), and neither of the beetle red ($p = 0.31$) nor beetle gray ($p = 0.15$) stands were significantly different from healthy stands, although the percent of gray phase tree was low (<20 %) in 2009.

### 3.2 Vegetation water and energy changes

While a large amount of mortality was noted, little change in environmental drivers of above canopy radiation (Fig. 2a), above canopy air temperature (Fig. 2b), and soil temperature (Fig. 2d) was seen between years. The timing and magnitude of diurnal variations in bole temperature from a representative gray phase tree from BB07 are shown in Fig. 3 as compared to above canopy air temperature. A combination of heat capacity of the bole as well as radiation and air temperatures drove this temperature difference as the tree cooled more slowly overnight and warmed more rapidly during the day, relative to air temperatures. Bole temperature in a representative live tree from BB09 reached a maximum ~3 h earlier than the air and had a wider diurnal range than the air temperature by ~4 °C. As shown in the inset of Fig. 3, bole minus air temperatures between BB07 (gray) at night and BB09 (green) during midday for the month of August 2010 were significantly different from each other ($p < 0.05$). When temperature records were averaged across the entire month, including variation due to synoptic weather, temperature differences were minimized but remained up to 2 °C ($p < 0.05$) between infected and live tree bole temperatures. This translates to 50 W $m^{-2}$ differences in biomass energy storage at the stand scale. Time series hysteresis analysis between tree bole temperatures and above canopy air temperatures shows maximum differences of 1 °C for live trees and 2 °C for dead (Fig. 4) showing that living tree boles are undergoing smaller changes in temperature over a 24-h period compared to the dead and dry tree boles. This is

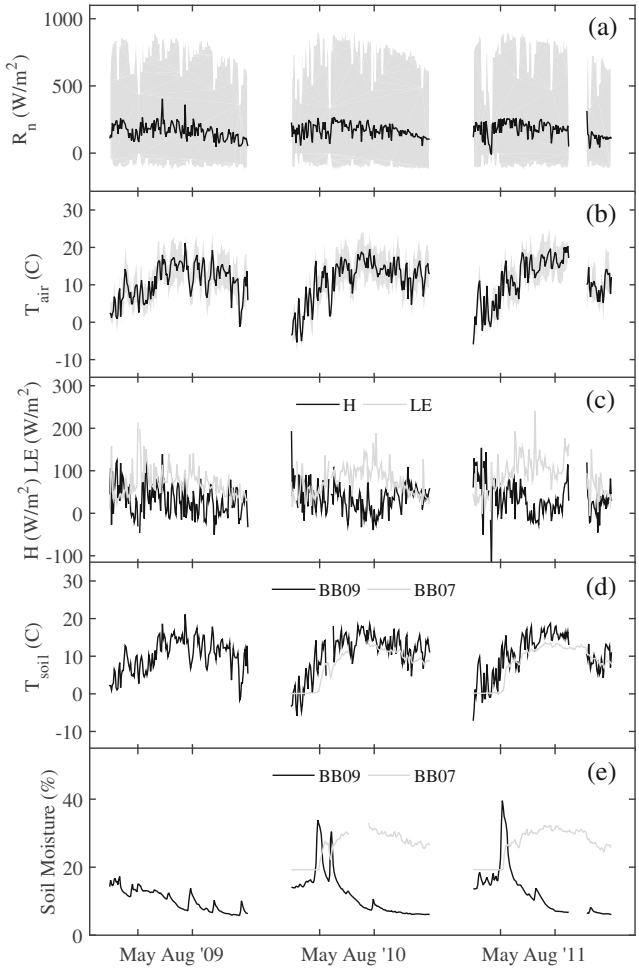


**Fig. 2** Seasonal variation in **a** mean net radiation with daily minimum and maximum values as shading at 17.1 m height, **b** mean air temperature at the BB09 stand with minimum and maximum values as shading at 17.7 m height, **c** sensible and latent heat flux at 17.7 m height, **d** soil temperature from BB09 and BB07 at 0.10 m depth, and **e** soil moisture from BB09 and BB07 integrated from 0.00 to 0.15 m depth during the growing seasons of 2009–2011. Data were averaged daily

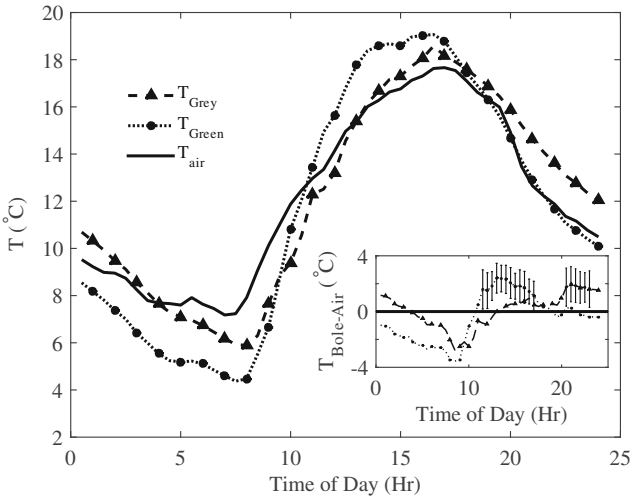


**Fig. 3** Average daily bole temperature at 1.3 m height and 0.02 m depth for infected (*gray*) and uninfected (*green*) trees in BB07 and BB09 as well as below canopy air temperature at 3.7 m height, averaged for August 2010. *Inset* is the difference between measured bole and air temperatures over the same time period, and *error bars* show for time periods where bole temperature is significantly different from air temperature

due to the higher water content of the living trees acting as a larger thermal mass relative to the dry boles. All tree boles are colder than air temperatures early in the day and warmer than air temperatures during late evening and early night.

Detailed 6-day temperature and energy storage are shown with a large change in location from canopy energy storage in low mortality stands and soil energy storage in high mortality stands in Fig. 4. We selected a 6-day time series that coincided with nearly clear skies throughout and a cold front passage during the period in order to illustrate impacts of air temperature changes (Fig. 5). Net radiation stayed high throughout the period, with only minimal afternoon clouds. There was a sharp decline in air temperatures on the seventh of September due to the frontal passage. This drove decreased vegetation energy storage in higher mortality stands as shown in Fig. 4h because of change to bole temperature measurements from the stands (Eq. 5). Maximum average energy storage within vegetation biomass of the impacted stand was half of that in the unimpacted stand, based primarily on thermodynamic differences between living tree boles with high water content and dry, dead tree boles (Figs. 3 and 4). Nighttime energy storage in an impacted stand was also half compared to an unimpacted stand, although in both stands, daily summed energy storage was not different significantly from zero based on 24-h averaging.

### 3.3 Soil water and energy changes

Given high mortality, soil moisture was on average 57 % higher (Fig. 2e) in the heavily impacted BB07 stand than in

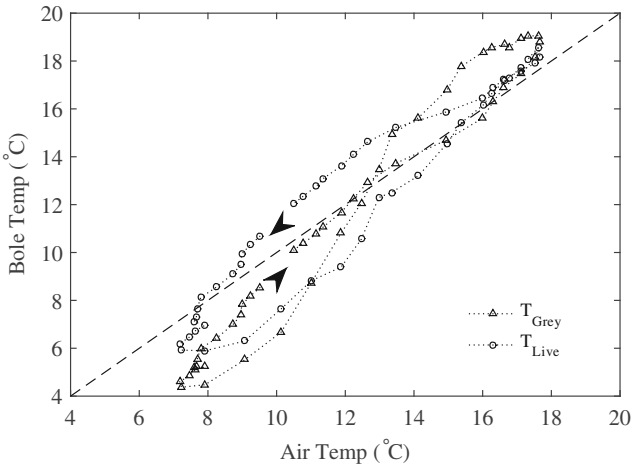


**Fig. 4** Average daily tree bole temperature at 1.3 m height and 0.02 m depth for infected (*gray*) and uninfected (*live*) tree boles compared to air temperature for the time period of August 2010. A 1:1 line is plotted for reference, and *arrows* show direction of hysteresis

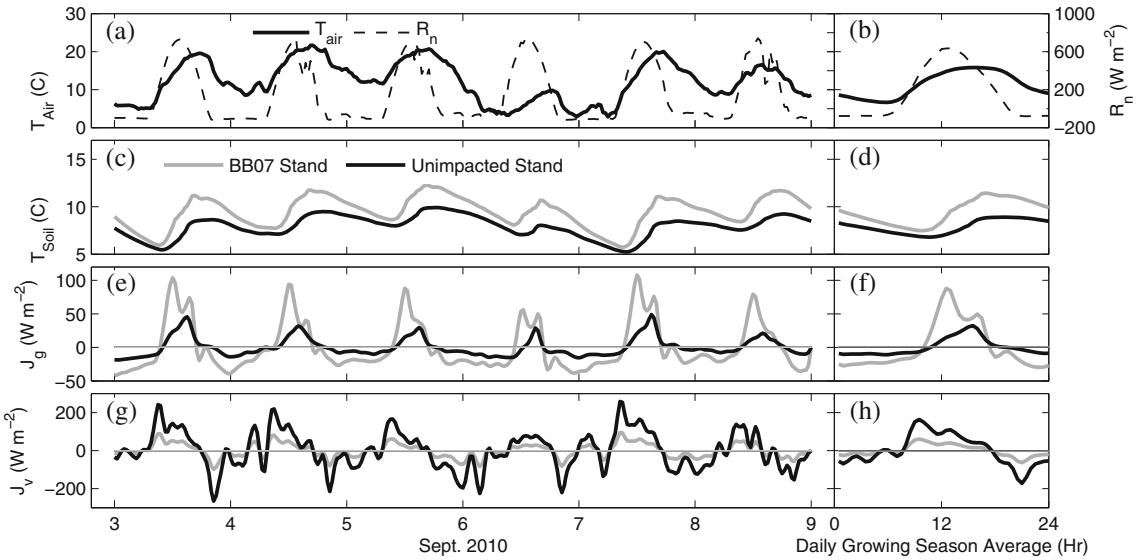


**Fig. 5** Abbreviated time series of **a** air temperature and net radiation, **c** soil temperature at BB07 and unimpacted stand, **e** soil energy storage, and **g** canopy vegetation energy storage. Diurnal average for the growing season of the same values shown in panels **b**, **d**, **f**, and **h**

the unimpacted stand for the entire growing season. At the end of the growing season, stand level soil moisture was lowest in intermediate mortality stands (BB09) at 7.95 %. Soil moisture increased in both stands responding to small rain events as expected, but soil moisture in the unimpacted stand decreased faster than in the impacted stand throughout the course of the study period (Fig. 2e).

Soil temperature was 1.5 °C higher in the high mortality BB07 stand (Fig. 2d). In the detailed 6-day time series (Fig. 5c, d), soil temperatures in both stands dropped following cold front passage, more so the following night due to clear skies and continued low air temperatures (Fig. 5a). Because there was a negligible drop in moisture (<0.1 %) over the 6-day period and no recorded rainfall, soil moisture is not shown.

Soil energy storage (Eq. 6) (Fig. 5f) shows a doubling of storage in the impacted stand, from both increased amplitude of diurnal soil temperatures (Fig. 5d) and increased soil moisture (Fig. 2e). As with vegetation energy storage, integrated over the course of 24 h, soil energy storage was not significantly different than zero ($p > 0.05$), meaning there was no net energy being stored in the soils over time scales longer than 1 day.

The relationship between eddy covariance water flux (LE) and soil water depletion ($\Delta\theta$) shows average agreement between water flux and soil water depletion, with a slope of 0.93 ($R^2 = 0.43$; $F = 6.69$) (Fig. 6). Time between rain events was highly variable, with many small precipitation events in 2009 compared with much longer time periods in between rain events in 2010 and 2011 (Fig. 2e). High soil water content values early in 2010 and 2011 (Fig. 2e) were due to late snowpack melt and were removed from this analysis due to large amounts of overland flow. Seasonally, daily averaged soil moisture (Fig. 7) showed little yearly variation between soil depths; however, the variation in soil moisture was larger in 2010 and 2011. Average soil moisture increased approximately 10 % between shallow and deep layers as expected.

On a seasonal time scale, averaged latent heat fluxes displayed good agreement with seasonal average soil moisture (Fig. 8a). Similar to soil moisture variability, the relationship between soil moisture and latent heat was more variable in 2010 (Fig. 8c) and 2011 (Fig. 8d).

### 3.4 Surface radiation changes

Plots of daily averaged latent heat flux by year (Fig. 9a) correspond primarily with inter-annual variability in soil water,

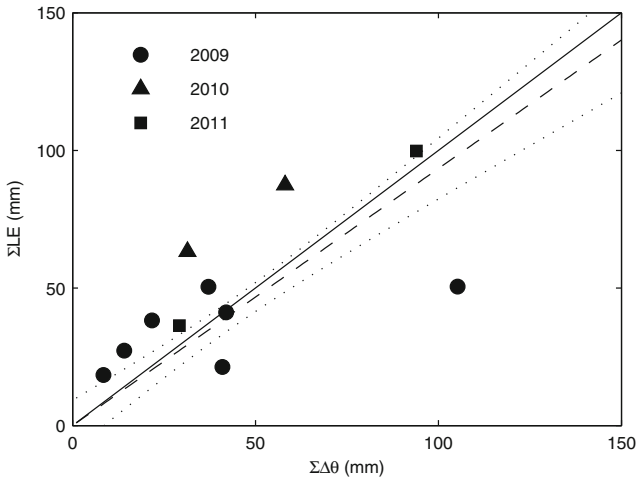


**Fig. 6** Sums of daily ecosystem water flux (ΣLE) flux plotted against sums of ecosystem soil moisture depletion (scaled from multiple stands) ($\Sigma\Delta\theta$) over each dry periods for each year. The solid line is a 1:1 line with the *dashed line* indicating the regression line and the 95 % confidence bands. Average summation length was 21 days with the minimum time between rain events was 7 days and the maximum 58 days.

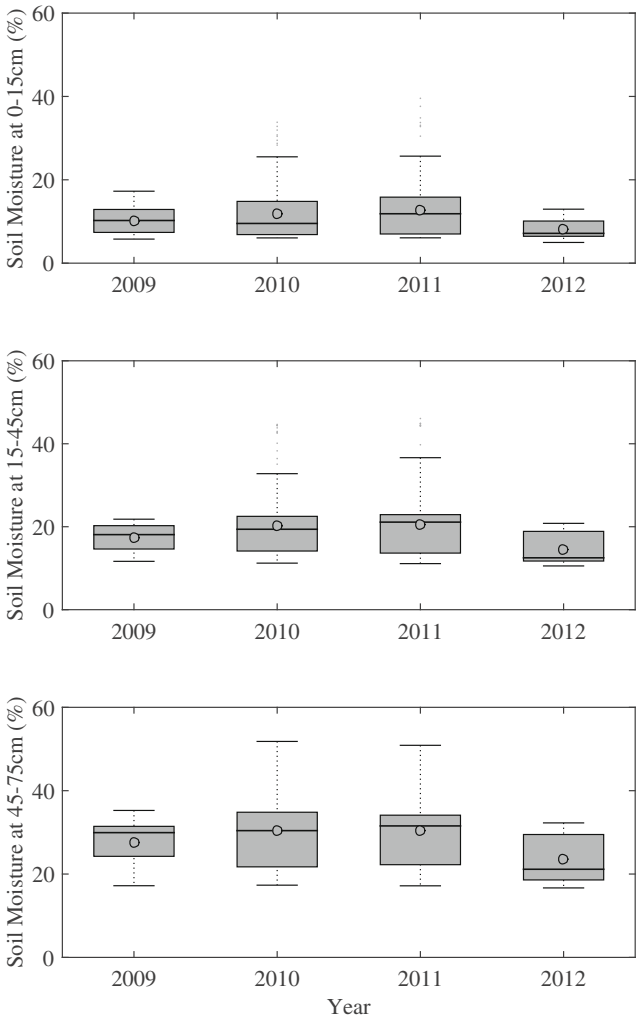


**Fig. 7** Daily averaged ecosystem soil moisture at depths of 0–15 cm (**a**), 15–45 cm (**b**), and 45–75 cm (**c**)

while sensible heat flux (Fig. 9b) was unchanged between years. Variability in latent heat was larger in 2010 and 2011, while variability in sensible heat did not change between years. The seasonally averaged Bowen ratio shows a large increase of approximately 0.4 in 2012 (Fig. 9c), which was record drought year across the USA (Hoerling et al., 2014), leading to low soil moisture and low latent flux.

Solar outgoing (ground to sky) radiation did not change between years (Fig. 10a) along with solar albedo (not shown) with maximum difference between years <4 W $m^{-2}$ $s^{-1}$. Variation in solar outgoing radiation was higher in 2010 and 2011. Longwave outgoing radiation increased in 2012 (Fig. 10b) and had large variability in 2011. Incoming solar and longwave radiation were similar between years (not shown). These changes in the components of the radiation budget largely canceled each other out, and net radiation was similar between years with 2011 variability being notable (Fig. 10c) due to high variability in the component radiation terms.

## 4 Discussion

In an even-aged lodgepole pine forest, 4 years after a mountain pine bark beetle outbreak, spatially heterogeneous tree mortality reached 78 % within the footprint (Fig. 1e). Within infected stands, mortality is expected to level off as the bark beetles do not have enough large diameter trees to act as suitable hosts for subsequent generations (Pelz and Smith 2012; Raffa et al. 2008; Reid 1962). Mortality under 100 % allows re-establishment of pine at a faster rate than other disturbance types such as clear-cutting, fire, blow-down, or avalanche (Oliver 1980; Rammig et al. 2006) and would have significant impacts on ecosystem and canopy mechanisms that control recovery. The percentage of the forest consisting of small diameter, non-suitable host trees was expected to vary between 5 and 20 % across the region based on forest surveys (Thompson et al. 2005).

As a result of beetle outbreak and tree mortality, variability in many ecosystem measurements was high in 2010 and 2011. Atmospheric latent heat flux, soil moisture, and radiation measurements all showed an increase in variability during the middle of the outbreak, when mortality levels were over 70 %, but before the understory regrew. Co-located soil nitrogen and methane fluxes (Norton et al. 2015) show disequilibrium for up to 5 years following disturbance, with staggered responses from different gas species. Inter-annual variability of soil respiration was comparable to the variability attributable to tree mortality across the same ecosystem during the same period (Borkhuu et al. 2015). A period of ecosystem transition was hypothesized (Edburg et al. 2012), and changes in multiple ecosystem processes during the disturbance are thought to be driving this increase in measured variation from soils to above the canopy.

Following our predictions of hypothesis 1 that moisture increases as the canopy dries following mortality, we see that soils in a stand that was unaffected by beetles were wet at the start of the growing season and dried over the course of the summer. When transpiration declines in a stand with high mortality like BB07 (Edburg et al. 2012; Mikkelson et al. 2013; Yamaoka et al. 1990), water cycling ends up being altered. As a result of the reduction in transpiration, we observed that tree boles and canopy biomass dried out and soil moisture remained high in stands with high mortality throughout the summer. In a stand with a mix of uninfected and infected trees (BB09), soil water content was lower than in the high mortality stand. Tree ring analyses (Romme et al. 1986) and basal area growth rates (Szwagrzyk and Szewczyk 2001) have shown that the surviving trees grow faster after release from competition, suggesting that stand level transpiration rates do not decline much in stands with >60 % surviving trees (Hubbard et al. 2013). With basal areas of surviving trees being positively correlated with the amount of recently dead basal area in a similar montane forest (Szwagrzyk and

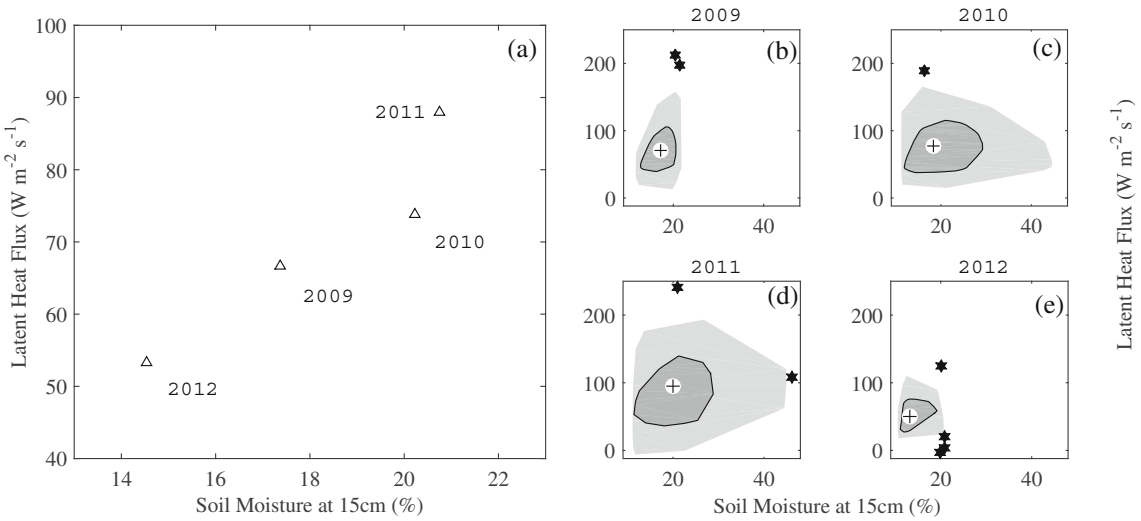


**Fig. 8** Seasonally averaged ecosystem soil moisture from all plots at 15 cm depth compared to seasonally averaged latent heat fluxes (**a**), with daily averaged bagplots (bivariate boxplots) of 2009 (**b**), 2010 (**c**), 2011 (**d**), and 2012 (**e**) shown separately, where the *cross* is the median of the dataset, the *dark shading* is the quartile range and contains 50 % of the dataset, the *light shading* contains all non-outliers (95 % of the dataset), and outliers are marked as *stars*

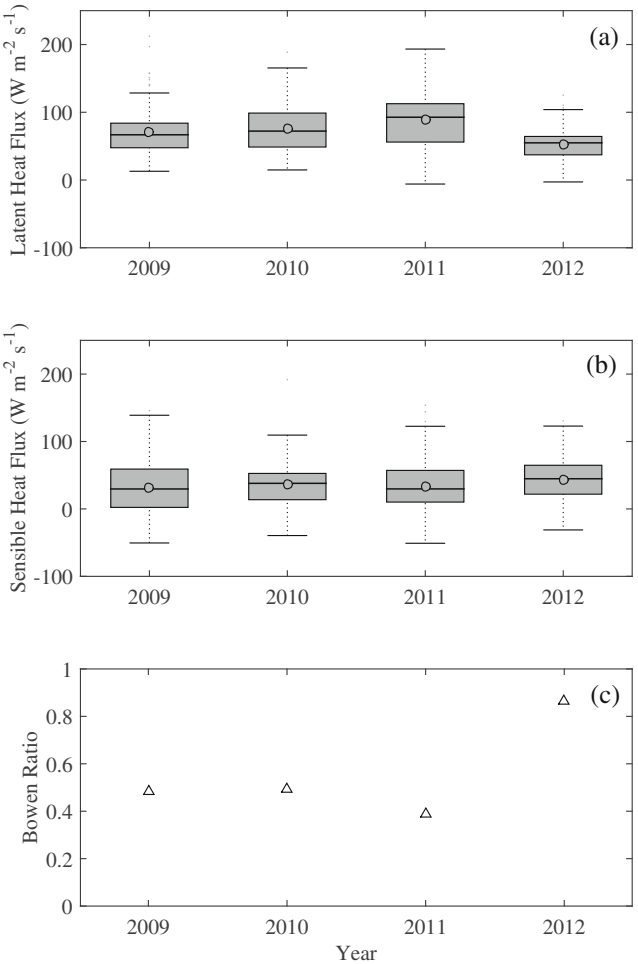


**Fig. 9** Daily averaged latent heat flux (**a**), sensible heat flux (**b**), and the seasonal Bowen Ratio for the ecosystem (**c**) observed from BB09 but representative of the ecosystem.

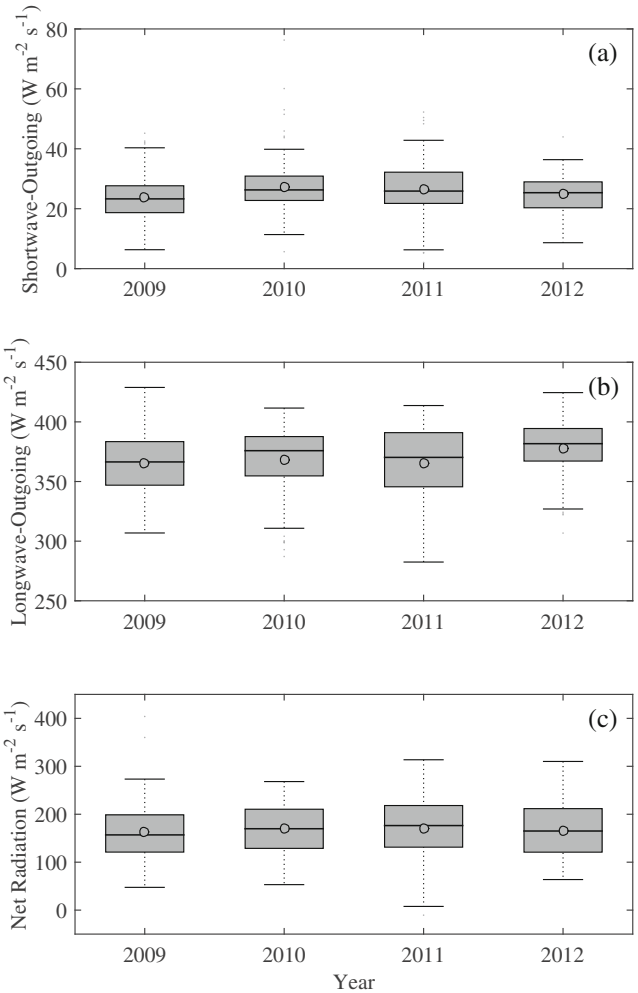


**Fig. 10** Daily averaged outgoing shortwave radiation (**a**), outgoing longwave radiation (**b**), and net radiation (**c**) from BB09

Szewczyk 2001), and the formation of root gaps only in clusters of less than 30 dead trees (Ponton et al., 2006), this may be the mechanism responsible for observed low soil water content in stands with mixed amounts of mortality.

Water budget changes in stands can also impact carbon and downstream watershed processes of the ecosystem. The results of Brown et al. (2010) and Frank et al. (2014) show remaining healthy trees and regenerating understory still uptake carbon and transpire water at similar rates. This was primarily due to the opening of the over-story canopy, allowing more light to the understory and surviving trees. Soil groundwater in stands as well as the contribution to streams from beetle-impacted stands has been shown to increase in late summer throughout beetle-impacted watersheds (Bearup et al. 2014).

Hypothesis number 2 predicted altered radiation fluxes at the site following changes in the canopy. As the canopy was expected to change first in color and then open, this would impact first outgoing shortwave radiation and then longwave radiation. However, in contrast to our expectations, we observed only an insignificant declining trend in LAI following beetle infestation. This is thought to be caused by the low number of gray needle phase trees in the high mortality stand at the time of sample and the remaining high amounts of non-leaf biomass (boles and branches) that are not expected to be impacted by bark beetles. Due to higher amounts of non-leaf biomass in coniferous canopies, statistically significant declines are unlikely to be observed, even when all needles are lost in a high mortality stand (Gower et al. 1999). If LAI continues to decline as expected (Edburg et al. 2012), increased solar radiation would reach the forest floor as observed in other studies (Brown et al. 2010; Pugh and Gordon 2013). Similar processes of canopy opening after disturbance are also noted in other deciduous forest mortality studies (Hardiman et al. 2013).

The observed changes of outgoing solar and longwave radiation of hypothesis 2 are potentially explained by canopy defoliation and support the conceptual predictions of Pugh and Gordon (2013). However, a more open canopy would mean the longwave radiation observations are dominated by longwave emissions from the soil surface and not the canopy surface. The soil surface is expected to be warmer. Hence, when the canopy opens, longwave emissions increase, opposite of what was predicted by Pugh and Gordon (2013). In this work, there were only small observed changes in outgoing shortwave and longwave radiation during the study and hypothesis 2 was largely rejected, with more change observed in the variability of radiation terms than the average amount of radiation. Scaling observations from a single stand to the ecosystem level model put forth by Pugh and Gordon (2013) remains a challenge.

The observed impacts on sensible and latent heat fluxes as well as the Bowen ratio of the site partially supported the predictions of hypothesis 3. Where we thought mortality would drive a decline in tree transpiration, instead we observed greater soil moisture evaporation contribution to the site's latent heat flux. Biederman et al. (2014b) showed water isotopic results that suggest evaporation is making up a larger component of the ecosystem water vapor flux, and Reed et al. (2014) modeled increasing ecosystem level canopy conductance following bark beetle mortality, suggesting more evaporation than transpiration at the ecosystem level. Without the observed decline in latent fluxes, the expected change in sensible heat did not follow. However, the increase in Bowen ratio at the site in 2012 partially confirms hypothesis 3 and may be explained by the mortality levels, combined with extreme warm and dry conditions for the year (Hoerling et al. 2014). Similar shifts in fluxes and Bowen ratio were observed in forested sites over a fire chronosequence, where post-fire regeneration was not uniform across the affected site (Liu et al. 2005). Latent heat fluxes should increase in sites that are recovering from fire due to high amounts of shrub and deciduous tree cover and the transpiration flux from the understory, while sensible heat fluxes decrease. However, in this study, we see an overall good agreement between seasonally averaged latent heat and soil moisture amounts and no increase in sensible heat as predicted by hypothesis 3. Previous studies have shown an increase in understory and soil evaporation response from bark beetles and very small total changes in latent heat fluxes (Brown et al. 2014; Reed et al. 2014).

Site water budget changes were observed as soil energy storage increased and canopy energy storage decreased 2 years after infestation at our study site. In a healthy stand, energy storage is normally high in the vegetation biomass, due to canopy light interception and water storage in tree boles. The canopy shades the dry soil, so energy storage is relatively low. After mortality, the two processes of declining transpiration and opening of the canopy end up causing more energy storage in soils and less in the canopy biomass.

The high levels of variability in measurements convey important information about the underlying ecosystem processes (Fraterrigo and Rusak 2008). In this study, variability of soil moisture, latent heat fluxes, and radiation terms all increased in the middle of the beetle outbreak, when mortality levels were the most heterogeneous across the landscape. Measuring and detecting variability in ecosystems processes require both temporal and spatial measurements (Turner et al. 1993). Combining multiple measurement techniques allows for the same process to be examined from different points of view, such as the opening of the canopy during a disturbance being quantified from an LAI, soil moisture, and energy storage angle. This gives greater insight into the duration of competing ecosystem processes, in a way that a single measurement often cannot.

## 5 Conclusions

Four years after initial bark beetle infestation, there was 78.4 % mortality at our lodgepole pine site in southeastern Wyoming. This mortality caused heterogeneity within the footprint of an eddy covariance tower and a redistribution of water from living tree boles to soil water. This altered the thermodynamic energy storage at the individual stands, increasing the energy storage in the soils and decreasing energy storage in the vegetation as the bark beetle outbreak continued. The total magnitude of water and energy storage was similar and tends to offset throughout the outbreak but was in different spatial locations, in biomass, and soil, respectively.

Seasonal latent heat fluxes were more dependent on interannual soil water and showed no correlation with mortality. Ecosystem transpiration was assumed to decline on an ecosystem scale and soil evaporation increased to compensate. A large increase in ecosystem Bowen ratio was noted in 2012 which corresponded to a dry (low latent heat) and high mortality year. Variability of soil, atmospheric flux, and radiation measurements were observed to be higher during the disturbance. As disturbances and ecosystem transitions become more likely in the future, ecosystems observations will become increasing variable. Instead of treating this variability as simply noise within the observation, quantifying variability will give greater insight to the organizing processes and a better understanding of the seeming randomness of disturbances. Only with an understanding of the causes of the variability can the underlining mechanisms be included in process models of ecosystem recovery after disturbance.

**Acknowledgments** We thank W. Massman and R. Leuning for constructive comments, J. Angstmann for assistance with data logger setup, C. Rumsey for her climbing experience, F. Whitehouse with sensor installation and dried biomass weights, Drew King with LAI data collection and processing, S. Peckham and G. Bolton for field site maintenance, and Yost R. for field processing of coarse woody debris samples. This chapter was written by D. Reed with edits by B. Ewers and E. Pendall, with additional analysis ideas supplied by J. Frank and R. Kelly. This work was funded by the National Science Foundation (GEO-1430396, EPS-1208909 and EAR-0910831), UW Agriculture Experiment Station, Wyoming Water Development Commission, the United States Geological Survey, and University of Wyoming NASA-EPSCoR.

## References

Allen CD et al (2010) A global overview of drought and heat-induced tree mortality reveals emerging climate change risks for forests. For Ecol Manag 259(4):660–684

Amiro, B.D. et al., 2010. Ecosystem carbon dioxide fluxes after disturbance in forests of North America. Journal of Geophysical Research-Biogeosciences, 115: G00 K02.

Asrar G, Myneni RB, Choudhury BJ (1992) Spatial heterogeneity in vegetation canopies and remote-sensing of absorbed photosynthetically active radiation—a modeling study. Remote Sens Environ 41(2–3):85–103

Baldocchi DD, Law BE, Anthoni PM (2000) On measuring and modeling energy fluxes above the floor of a homogeneous and heterogeneous conifer forest. Agric For Meteorol 102(2–3):187–206

Baldocchi D et al (2001) FLUXNET: a new tool to study the temporal and spatial variability of ecosystem-scale carbon dioxide, water vapor, and energy flux densities. Bull Am Meteorol Soc 82(11):2415–2434

Bearup LA, Maxwell RM, Clow DW, McCray JE (2014) Hydrological effects of forest transpiration loss in bark beetle-impacted watersheds. Nature Clim Change 4(6):481–486

Bergeron Y, Leduc A, Joyal C, Morin H (1995) Balsam fir mortality following the last spruce budworm outbreak in northwestern Quebec. Can J For Res 25(8):1375–1384

Biederman JA et al (2014a) Multiscale observations of snow accumulation and peak snowpack following widespread, insect-induced lodgepole pine mortality. Ecohydrology 7(1):150–162

Biederman JA et al (2014b) Increased evaporation following widespread tree mortality limits streamflow response. Water Resour Res 50(7): 5395–5409

Biederman JA et al (2015) Recent tree die-off has little effect on streamflow in contrast to expected increases from historical studies. Water Resour Res 51(12):9775–9789

Borkhuu B, Peckham SD, Ewers BE, Norton U, Pendall E (2015) Does soil respiration decline following bark beetle induced forest mortality? Evidence from a lodgepole pine forest. Agric For Meteorol 214–215:201–207

Bowen IS (1926) The ratio of heat losses by conduction and by evaporation from any water surface. Phys Rev 27(6):779–787

Brown M et al (2010) Impact of mountain pine beetle on the net ecosystem production of lodgepole pine stands in British Columbia. Agric For Meteorol 150(2):254–264

Brown MG et al (2012) The carbon balance of two lodgepole pine stands recovering from mountain pine beetle attack in British Columbia. Agric For Meteorol 153:82–93

Brown MG et al (2014) Evapotranspiration and canopy characteristics of two lodgepole pine stands following mountain pine beetle attack. Hydrol Process 28(8):3326–3340

Burrows SN et al (2002) Application of geostatistics to characterize leaf area index (LAI) from flux tower to landscape scales using a cyclic sampling design. Ecosystems 5(7):667–679

Edburg SL et al (2012) Cascading impacts of bark beetle-caused tree mortality on coupled biogeophysical and biogeochemical processes. Front Ecol Environ 10(8):416–424

Ewers BE, Oren R, Albaugh TJ, Dougherty PM (1999) Carry-over effects of water and nutrient supply on water use of *Pinus taeda*. Ecol Appl 9(2):513–525

Finnigan JJ, Clement R, Malhi Y, Leuning R, Cleugh HA (2003) A re-evaluation of long-term flux measurement techniques part I: averaging and coordinate rotation. Bound-Layer Meteorol 107(1):1–48

Flannigan MD, Logan KA, Amiro BD, Skinner WR, Stocks BJ (2005) Future area burned in Canada. Clim Chang 72(1–2):1–16

Frank JM, Massman WJ, Ewers BE, Huckaby LS, Negrón JF (2014) Ecosystem CO2/H2O fluxes are explained by hydraulically limited gas exchange during tree mortality from spruce bark beetles. Journal of Geophysical Research: Biogeosciences 119(6):1195–1215

Fraterrigo JM, Rusak JA (2008) Disturbance-driven changes in the variability of ecological patterns and processes. Ecol Lett 11(7):756–770

Gower ST, Kucharik CJ, Norman JM (1999) Direct and indirect estimation of leaf area index, fAPAR, and net primary production of terrestrial ecosystems. Remote Sens Environ 70(1):29–51

Gu LH et al (2005) Objective threshold determination for nighttime eddy flux filtering. Agric For Meteorol 128(3–4):179–197

Hardiman B, Bohrer G, Gough C, Curtis P (2013) Canopy structural changes following widespread mortality of canopy dominant trees. Forests 4(3):537–552

Hoerling M et al (2014) Causes and predictability of the 2012 Great Plains drought. Bull Am Meteorol Soc 95(2):269–282

Hopping GR, Beall G (1948) The relation of diameter of lodgepole pine to incidence of attack by the bark beetle Dendroctonus monticolae Hopkins. For Chron 24(2):141–145

Horst TW (2000) On frequency response corrections for Eddy covariance flux measurements. Bound-Layer Meteorol 94(3):517–520

Horst T, Lenschow D (2009) Attenuation of scalar fluxes measured with spatially-displaced sensors. Bound-Layer Meteorol 130(2):275–300

Hubbard RM, Rhoades CC, Elder K, Negron J (2013) Changes in transpiration and foliage growth in lodgepole pine trees following mountain pine beetle attack and mechanical girdling. For Ecol Manag 289:312–317

Knight DH, Fahey TJ, Running SW (1985) Water and nutrient outflow from contrasting lodgepole pine forests in Wyoming. Ecol Monogr 55(1):29–48

Kurz WA et al (2008a) Mountain pine beetle and forest carbon feedback to climate change. Nature 452(7190):987–990

Kurz WA, Stinson G, Rampley GJ, Dymond CC, Neilson ET (2008b) Risk of natural disturbances makes future contribution of Canada's forests to the global carbon cycle highly uncertain. Proc Natl Acad Sci U S A 105(5):1551–1555

Lee X, Massman W, Law B (2004) Handbook of micrometeorology: a guide for surface flux measurement and analysis. In: Atmospheric and oceanographic sciences library, 29. Kluwer, Dordrecht

Liu HP, Randerson JT, Lindfors J, Chapin FS (2005) Changes in the surface energy budget after fire in boreal ecosystems of interior Alaska: an annual perspective. J Geophys Res-Atmos 110(D13): D13101

Loescher HW, Hanson CV, Ocheltree TW (2009) The psychometric constant is not constant: a novel approach to enhance the accuracy and precision of latent energy fluxes through automated water vapor calibrations. J Hydrometeorol 10(5):1271–1284

Mackay DS et al (2002) Effects of aggregated classifications of forest composition on estimates of evapotranspiration in a northern Wisconsin forest. Glob Chang Biol 8(12):1253–1265

Man RZ, Rice JA (2010) Response of aspen stands to forest tent caterpillar defoliation and subsequent overstory mortality in northeastern Ontario, Canada. For Ecol Manag 260(10):1853–1860

Massman WJ (2000) A simple method for estimating frequency response corrections for eddy covariance systems. Agric For Meteorol 104(3):185–198

McCaughey JH (1985) Energy-balance storage terms in a mature mixed forest at PETAWAWA, Ontario—a case-study. Bound-Layer Meteorol 31(1):89–101

McNulty SG, Aber JD, Newman SD (1996) Nitrogen saturation in a high elevation New England spruce-fir stand. For Ecol Manag 84(1–3): 109–121

Meyers TP, Hollinger SE (2004) An assessment of storage terms in the surface energy balance of maize and soybean. Agric For Meteorol 125(1–2):105–115

Mikkelson K et al (2013) Bark beetle infestation impacts on nutrient cycling, water quality and interdependent hydrological effects. Biogeochemistry 115(1–3):1–21

Minckley TA, Shriver RK, Shuman B (2012) Resilience and regime change in a southern Rocky Mountain ecosystem during the past 17 000 years. Ecol Monogr 82(1):49–68

Moncrieff JB, Malhi Y, Leuning R (1996) The propagation of errors in long-term measurements of land-atmosphere fluxes of carbon and water. Glob Chang Biol 2(3):231–240

Monin AS, Obukhov AM (1954) Basic laws of turbulence mixing in the ground layer of the atmosphere. Acad Nauk SSR Trud Geofiz Inst 24:163–187

Negrón JF, Popp JB (2004) Probability of ponderosa pine infestation by mountain pine beetle in the Colorado Front Range. For Ecol Manag 191(1–3):17–27

Niinemets U (2010) Responses of forest trees to single and multiple environmental stresses from seedlings to mature plants: past stress history, stress interactions, tolerance and acclimation. For Ecol Manag 260(10):1623–1639

Norton U, Ewers BE, Borkhuu B, Brown NR, Pendall E (2015) Soil nitrogen five years after bark beetle infestation in lodgepole pine forests. Soil Sci Soc Am J 79(1):282–293

Oliver CD (1980) Forest development in North America following major disturbances. For Ecol Manag 3:153–168

Panek JA, Kurpius MR, Goldstein AH (2002) An evaluation of ozone exposure metrics for a seasonally drought-stressed ponderosa pine ecosystem. Environ Pollut 117(1):93–100

Pearson JA, Fahey TJ, Knight DH (1984) Biomass and leaf-area in contrasting lodgepole pine forests. Canadian Journal of Forest Research-Revue Canadienne De Recherche Forestiere 14(2):259–265

Pelz KA, Smith FW (2012) Thirty year change in lodgepole and lodgepole/mixed conifer forest structure following 1980s mountain pine beetle outbreak in western Colorado, USA. For Ecol Manag 280:93–102

Ponton S et al (2006) Comparison of ecosystem water-use efficiency among Douglas-fir forest, aspen forest and grassland using eddy covariance and carbon isotope techniques. Glob Chang Biol 12(2): 294–310

Potts DF (1984) Hydrologic impacts of a large-scale mountain pine-beetle (Dendroctonus ponderosae Hopkins) epidemic. Water Resour Bull 20(3):373–377

Prescott CE (2002) The influence of the forest canopy on nutrient cycling. Tree Physiol 22(15–16):1193–1200

Pugh E, Gordon E (2013) A conceptual model of water yield effects from beetle-induced tree death in snow-dominated lodgepole pine forests. Hydrol Process 27(14):2048–2060

Pugh E, Small E (2012) The impact of pine beetle infestation on snow accumulation and melt in the headwaters of the Colorado River. Ecohydrology 5(4):467–477

Raffa KF et al (2008) Cross-scale drivers of natural disturbances prone to anthropogenic amplification: the dynamics of bark beetle eruptions. Bioscience 58(6):501–517

Rammig A, Fahse L, Bugmann H, Bebi P (2006) Forest regeneration after disturbance: a modelling study for the Swiss Alps. For Ecol Manag 222(123):–136

Reed DE, Ewers BE, Pendall E (2014) Impact of mountain pine beetle induced mortality on forest carbon and water fluxes. Environ Res Lett 9(10):105004

Reid RW (1962) Biology of the mountain pine beetle, Dendroctonus monticolae Hopkins, in the East Kootenay Region of British Columbia I. Life cycle, brood development, and flight periods. The Canadian Entomologist 94(5):531–538

Rhoades, C.C. et al., 2013. Biogeochemistry of beetle-killed forests: explaining a weak nitrate response. Proceedings of the National Academy of Sciences

Romme WH, Knight DH, Yavitt JB (1986) Mountain pine beetle outbreaks in the Rocky Mountains: regulators of primary productivity? Am Nat 127(4):484–494

Rousseeuw PJ, Ruts I, Tukey JW (1999) The bagplot: a bivariate boxplot. Am Stat 53(4):382–387

Safranyik L et al (2010) Potential for range expansion of mountain pine beetle into the boreal forest of North America. Can Entomol 142(5): 415–442

Schuepp PH, Leclerc MY, MacPherson JI, Desjardins RL (1990) Footprint prediction of scalar fluxes from analytical solutions of the diffusion equation. Bound-Layer Meteorol 50(1):355–373

Szwagrzyk J, Szewczyk J (2001) Tree mortality and effects of release from competition in an old-growth Fagus-Abies-Picea stand. J Veg Sci 12(5):621–626

Thompson, M.T., DeBlander Larry T., Blackard Jock A., 2005. Wyoming's forests, 2002. Resour. Bull. RMRS-RB-6. Fort Collins,

Department of Agriculture, Forest Service, Rocky Mountain Research Station. 148 p.

Tingey DT et al (2001) Elevated CO2 and temperature alter the response of *Pinus ponderosa* to ozone: a simulation analysis. Ecol Appl 11(5):1412–1424

Turner MG (1989) Landscape ecology: the effect of pattern on process. Annu Rev Ecol Syst 20:171–197

Turner MG, Romme WH, Gardner RH, O'Neill RV, Kratz TK (1993) A revised concept of landscape equilibrium: disturbance and stability on scaled landscapes. Landsc Ecol 8(3):213–227

Tymstra C, Flannigan MD, Armitage OB, Logan K (2007) Impact of climate change on area burned in Alberta's boreal forest. Int J Wildland Fire 16(2):153–160

van Mantgem PJ et al (2009) Widespread increase of tree mortality rates in the western United States. Science 323(5913):521–524

Webb EK, Pearman GI, Leuning R (1980) Correction of flux measurements for density effects due to heat and water vapour transfer. Q J R Meteorol Soc 106(447):85–100

Westerling AL, Hidalgo HG, Cayan DR, Swetnam TW (2006) Warming and earlier spring increase western US forest wildfire activity. Science 313(5789):940–943

Yamaoka Y, Swanson RH, Hiratsuka Y (1990) Inoculation of lodgepole pine with four blue-stain fungi associated with mountain pine beetle, monitored by a heat pulse velocity (HPV) instrument. Can J For Res 20(1):31–36